

X-ray Spectroscopy and Variability of AGN Detected in the 2 Ms Chandra Deep Field-North Survey

F.E. Bauer,¹ C. Vignali,¹ D.M. Alexander,¹ W.N. Brandt,¹ G.P. Garmire,¹ A.E. Hornschemeier,¹
P.S. Broos,¹ L.K. Townsley,¹ and D.P. Schneider¹

¹*Department of Astronomy & Astrophysics, 525 Davey Lab, The Pennsylvania State University, University Park, PA 16802*

ABSTRACT

We investigate the nature of the faint X-ray source population through X-ray spectroscopy and variability analyses of 136 AGN detected in the 2 Ms Chandra Deep Field-North survey with > 200 background-subtracted 0.5–8.0 keV counts [$F_{0.5-8.0 \text{ keV}} = (1.4-200) \times 10^{-15} \text{ erg cm}^{-2} \text{ s}^{-1}$]. Our preliminary spectral analyses yield median spectral parameters of $\Gamma = 1.61$ and intrinsic $N_{\text{H}} = 6.2 \times 10^{21} \text{ cm}^{-2}$ ($z = 1$ assumed when no redshift available) when the AGN spectra are fitted with a simple absorbed power-law model. However, considerable spectral complexity is apparent (e.g., reflection, partial covering) and must be taken into account to model the data accurately. Moreover, the choice of spectral model (i.e., free vs. fixed photon index) has a pronounced effect on the derived N_{H} distribution and, to a lesser extent, the X-ray luminosity distribution. Ten of the 136 AGN ($\approx 7\%$) show significant Fe K α emission-line features with equivalent widths in the range 0.1–1.3 keV. Two of these emission-line AGN could potentially be Compton thick (i.e., $\Gamma < 1.0$ and large Fe K α equivalent width). Finally, we find that 81 ($\approx 60\%$) of the 136 AGN show signs of variability, and that this fraction increases significantly ($\approx 80-90\%$) when better photon statistics are available.

INTRODUCTION

With the bulk of the $\approx 0.5-10.0$ keV background now resolved into discrete point sources (e.g., Mushotzky et al., 2000; Brandt et al., 2001; Rosati et al., 2002), emphasis has shifted toward determining the nature of the faint X-ray population — a clear necessity if we wish to understand the formation and evolution of active galactic nuclei (AGN). X-ray spectroscopy and variability analyses can play a crucial role in constraining the physical processes which occur in these AGN. For instance, the numerous X-ray spectroscopic and variability studies made prior to the launches of *Chandra* and *XMM-Newton* have found that (1) AGN X-ray spectra often show signs of complex absorption, reflection, and emission lines in addition to their power-law continuum radiation (e.g., Nandra and Pounds, 1994; Smith and Done, 1996; Lawson and Turner, 1997; Nandra et al., 1997b; Turner et al., 1997; George et al., 2000; Reeves and Turner, 2000), (2) the strengths of these spectral features (especially the reflection and emission components) depend on luminosity (e.g., Iwasawa and Taniguchi, 1993; Nandra et al., 1997c), and (3) a large fraction of AGN demonstrate variability of either continuum emission or absorption (e.g., Nandra et al., 1997a; Turner et al., 1999; Almaini et al., 2000; Grupe et al., 2001; Manners et al., 2002; Risaliti et al., 2002). However, these studies have generally focused on small samples of bright objects ($> 1 \times 10^{-13} \text{ erg cm}^{-2} \text{ s}^{-1}$), which are comprised of either nearby, moderate-luminosity AGN or rare, high-luminosity AGN at large look-back times. The deepest observations performed by *Chandra* and *XMM-Newton* now present the opportunity to study AGN ~ 100 times fainter in similar detail and thus place constraints on moderate-luminosity AGN at earlier epochs. Here we report on the spectral and temporal properties of the AGN in the 2 Ms exposure of the *Chandra* Deep Field-North (CDF-N), which probes $\approx 2-10$ times fainter in the 0.5–8.0 keV band than any other *Chandra* or *XMM-Newton* survey, and at least 50 and 250 times fainter than any past X-ray instrument in the 0.5–2.0 keV and 2.0–8.0 keV bands, respectively.

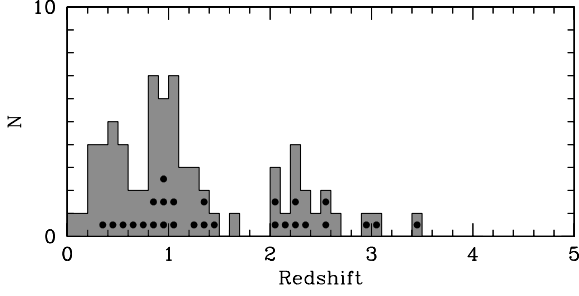


Fig. 1. Redshift distribution for the 72 sources in the sample with spectroscopic redshifts. Black dots indicate the sources which are confirmed broad-line AGN (Cohen et al., 2000; Barger et al., 2002).

DATA

Our sample was selected to ensure that we have adequate photon statistics for spectral and temporal analyses and is comprised of the 136 extragalactic X-ray sources with more than 200 background-subtracted, 0.5–8.0 keV counts in the 2 Ms CDF-N catalog (out of 503 total; Alexander et al., 2003b); X-ray spectral analyses of a few fainter X-ray sources are presented in Vignali et al. (2002) and Alexander et al. (2003a). With 0.5–8.0 keV fluxes ranging from 1.4×10^{-15} to 2×10^{-13} erg cm $^{-2}$ s $^{-1}$, these sources are characteristic of the population which comprises the bulk of the X-ray background below 10 keV. Seventy-two ($\approx 53\%$) of the sources in the sample have spectroscopic redshifts (see Figure 1); among these, nearly all have X-ray luminosities consistent with AGN. Based on their spectral slopes and X-ray-to-optical flux ratios (i.e., most have $I > 23$), the remaining unidentified sources are likely to be optically faint, obscured AGN at $z \sim 1$ –3 (e.g., Alexander et al., 2001; Barger et al., 2001). Thus almost all of the 136 sources appear to be AGN. Since the unidentified sources comprise almost half of the sample and may play an important role in the overall intrinsic column density and luminosity distributions, we have placed the unidentified sources at $z = 1$ (i.e., the likely lower redshift bound for these sources).

SPECTRAL ANALYSIS

Details of our spectral analysis procedure are given in Bauer et al. (2003). X-ray spectral fitting was performed using XSPEC (v11.2; Arnaud, 1996). We initially fitted each source with a simple model (hereafter MODEL 1) consisting of fixed Galactic photoelectric absorption ($N_{\text{H,GAL}} = 1.6 \times 10^{20}$ cm $^{-2}$ toward the CDF-N), a varying intrinsic N_{H} (using the redshift if known), and a power law with varying photon index (Γ). Approximately 75% of the sources are acceptably fit by MODEL 1 [$P(\chi^2|\nu) < 0.05$]. Example spectra of two typical CDF-N AGN are shown in Figure 2. The MODEL 1 fits yield median spectral parameters of $\Gamma = 1.61$ and $N_{\text{H}} = 6.2 \times 10^{21}$ cm $^{-2}$ for our 136 sources, with large dispersions for both parameters; the overall distributions are shown in Figure 3. Note that the changes in these parameters are much less than their dispersions if we limit ourselves to the sources with redshifts (i.e., $\Gamma = 1.67$ and $N_{\text{H}} = 1.8 \times 10^{21}$ cm $^{-2}$) or with > 500 counts (i.e., $\Gamma = 1.69$ and $N_{\text{H}} = 3.2 \times 10^{21}$ cm $^{-2}$). The N_{H} distribution has a peak at $N_{\text{H}} \approx \text{Galactic}$, and very few objects ($< 9\%$) have $N_{\text{H}} > 10^{23}$ cm $^{-2}$. The 27 optically identified broad-line AGN (BLAGN) appear to trace the same N_{H} distribution as the overall sample. The typical photon indices found for the CDF-N AGN are $\Delta\Gamma \sim 0.2$ –0.3 lower than the canonical intrinsic X-ray spectral slope value of AGN (e.g., $\Gamma \sim 1.9$ –2.0; Nandra and Pounds, 1994; Brandt et al., 1997; Reeves and Turner, 2000), suggesting the presence of additional spectral complexity (e.g., reflection, complex intrinsic absorption, partial covering). This fact is strengthened somewhat by the systematic residuals (e.g., soft excesses, spectral curvature) seen in several objects.

Detailed modeling of this complexity is underway but is beyond the scope of this paper. As a simple test of how the N_{H} and L_{X} distributions could be affected by spectral complexity, we fitted the data with a model identical to MODEL 1, but with the photon index fixed to $\Gamma = 2$ (i.e., close to the canonical intrinsic slope found locally; hereafter MODEL 2). We find that fewer sources are acceptably fit [$P(\chi^2|\nu) < 0.05$] with MODEL 2 ($\approx 60\%$) and many sources have strong systematic residuals; this again suggests that there is spectral complexity. The median intrinsic absorption is $N_{\text{H}} = 1.5 \times 10^{22}$ cm $^{-2}$ and the median differences between intrinsic N_{H} and L_{X} for MODEL 1 and MODEL 2 are factors of 2.5 and 0.5, respectively (see Figure 4). The decrease in X-ray luminosity found for MODEL 2 is due in part to K -correction differences from the free versus fixed photon indices; note that the intrinsic X-ray luminosity could increase substantially if reflection and scattering were actually taken into account.

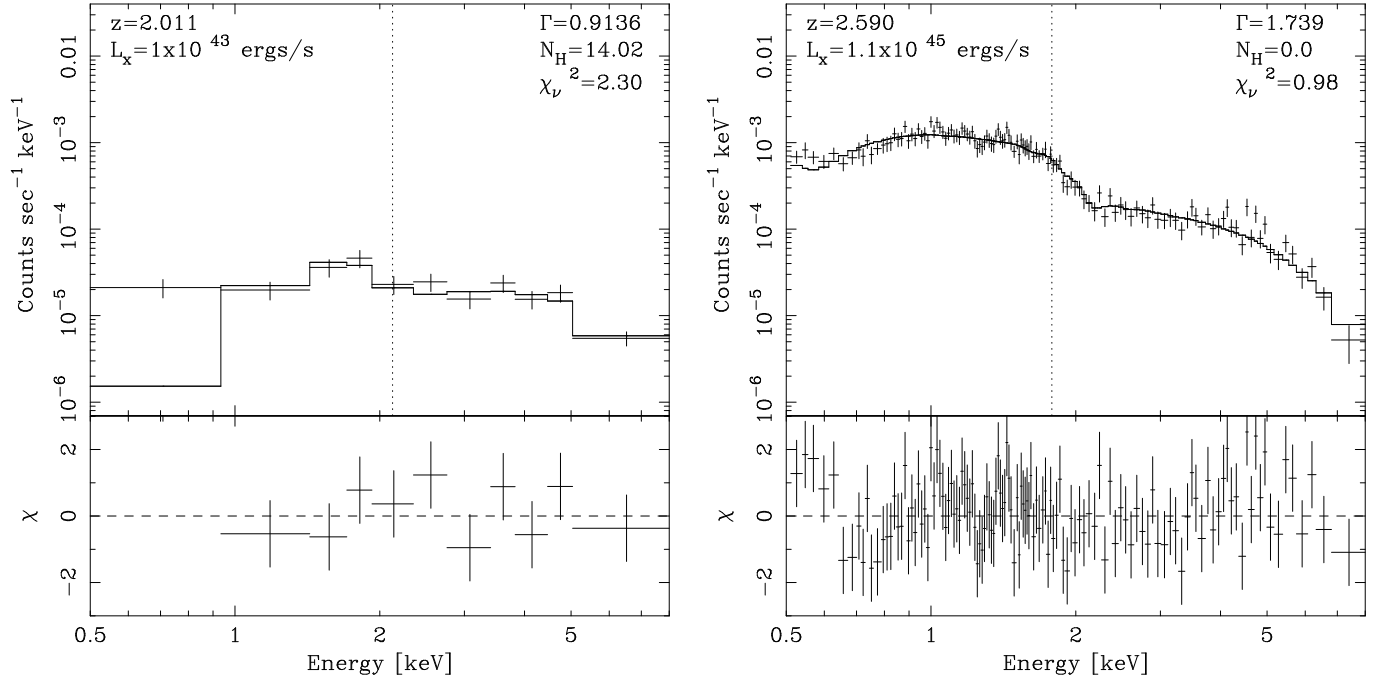


Fig. 2. Two example X-ray spectra fit with MODEL 1. The top panel shows a model fit to the data plotted in the observed-frame energy, while the bottom panel shows the residuals plotted in terms of χ . The relevant spectral fit parameters are shown inset (N_{H} is given in units of 10^{20} cm^{-2}). The vertical dotted line indicates the energy of the 6.4 keV Fe $K\alpha$ line at the source redshift. **Left:** CXOHDFN 123635.6+621424, an X-ray obscured Seyfert 2 galaxy (see also Dawson et al., 2001). **Right:** CXOHDFN 123622.9+621527, an unobscured quasar.

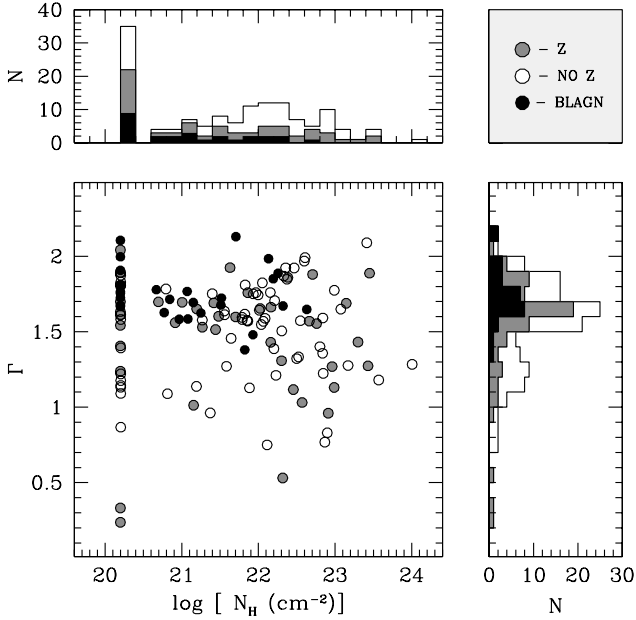


Fig. 3. Intrinsic N_{H} versus Γ (and their distributions) for the 136 X-ray sources in our sample fit with MODEL 1. Sources without redshifts are taken to have $z = 1$.

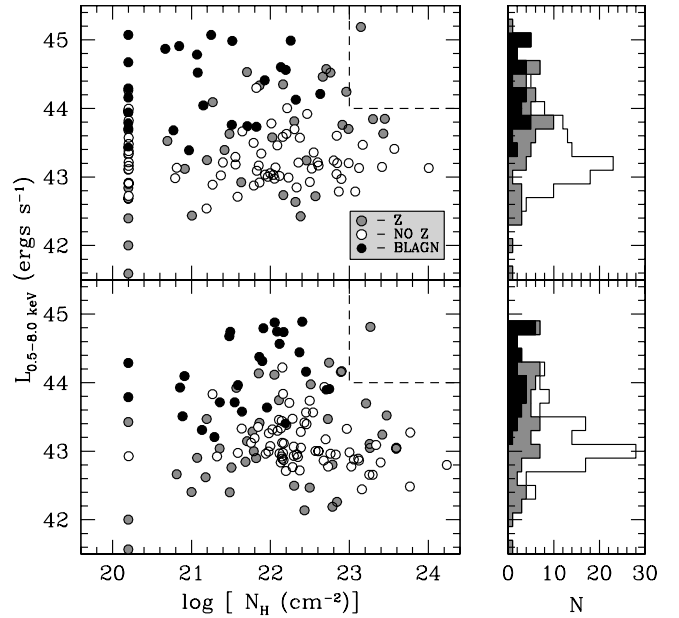


Fig. 4. Intrinsic N_{H} versus L_{X} for the 136 X-ray sources in our sample fit with MODEL 1 (**top**) and MODEL 2 (**bottom**). Sources without redshifts are taken to have $z = 1$. The dashed lines indicate the approximate region where obscured quasars should lie.

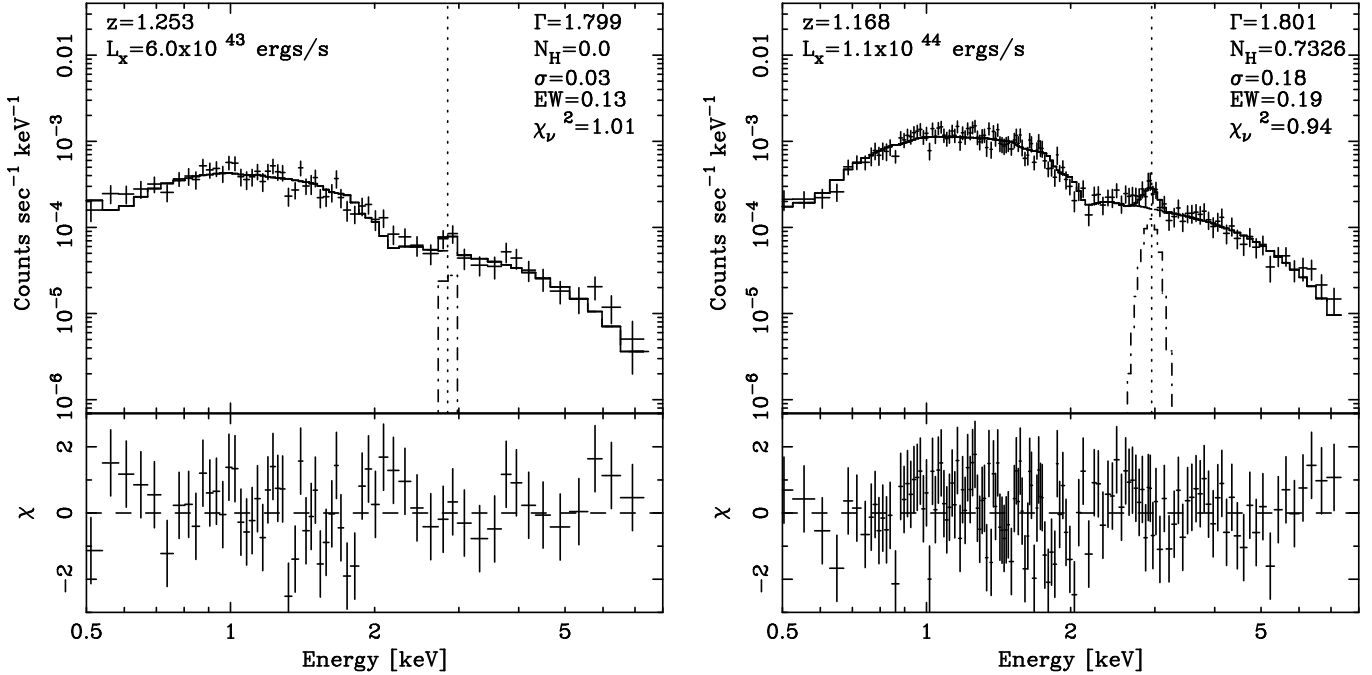


Fig. 5. Two example emission-line X-ray spectra fit with MODEL 1 plus a Gaussian emission line. See the Figure 2 caption for explanation (note N_H , σ , and EW are given in units of 10^{20} cm^{-2} , keV, and keV, respectively). **Left:** CXOHDFN 123704.1+620756, a BLAGN with a narrow emission line. **Right:** CXOHDFN 123740.9+621201, an obscured AGN with a mildly broadened or complex emission line.

EMISSION LINES

X-ray background synthesis models and X-ray spectral analyses of nearby sources both suggest that a large fraction of AGN may be Compton thick (e.g., Comastri et al., 1995; Risaliti et al., 1999), with direct emission observable only above rest-frame energies of ~ 10 keV (if at all). Below this energy, these AGN can only be detected via their faint reflected or scattered emission, typically in the form of extremely flat spectral slopes and large equivalent-width (EW) emission lines (e.g., Maiolino et al., 1998; Matt et al., 2000). We can place constraints on the existence of such objects at faint X-ray fluxes by searching for these features in our sample. For instance, 10 of the 136 AGN ($\approx 7\%$) exhibit obvious Fe K α emission-line features with $\text{EW} = 0.1\text{--}1.3$ keV. The emission lines appear to be typically a combination of narrow 6.4, 6.7, and 6.96 keV emission lines, although a few objects exhibit a possible broad wing redward of the 6.4 keV line. Example spectra of two typical CDF-N emission-line AGN are shown in Figure 5. Two of the emission-line sources are potentially Compton-thick AGN with $\Gamma < 1.0$ and $\text{EW} = 0.6\text{--}0.7$ keV. We can place further constraints on the number of reflection-dominated Compton-thick AGN in two ways. First, only 11 of the 136 sources have measured photon indices $\Gamma < 1.0$, suggesting that few objects in the sample show the signature of pure reflection that is characteristic of reflection-dominated Compton-thick AGN. Second, by modeling a Gaussian component to the source spectrum ($E = 6.4$ keV, $\sigma = 0$ keV), we can place upper limits on the Fe K α EWs for the 72 objects with redshifts. The range of Fe K α EW upper limits is 0.1–2.9 keV (i.e., consistent with local Seyferts; e.g., Nandra and Pounds, 1994), indicating that many sources may have emission lines which are still individually undetectable with the current data. However, only 8 of the 72 sources ($\approx 11\%$) have 90% confidence EW upper limits above 1 keV, and, of these, none has a measured photon index $\Gamma < 1.0$. Given that $\sim 50\%$ of all known Compton-thick sources have $\Gamma < 1.0$ and $\text{EW} > 1$ keV (e.g., Maiolino et al., 1998; Bassani et al., 1999), and that large EWs can also arise from anisotropic ionizing radiation or lags between continuum and line variability, the true number of Compton-thick AGN among our sample is likely to be small.

VARIABILITY

The 20 individual CDF-N observations span ≈ 27 months and offer an unprecedented probe of X-ray variability in distant AGN. Using Kolmogorov-Smirnov (single observations, second-to-day timescales) and χ^2 (multiple observations, day-to-year timescales) tests, we find that $\sim 55\%$ and $\sim 60\%$ of the 136 sources are

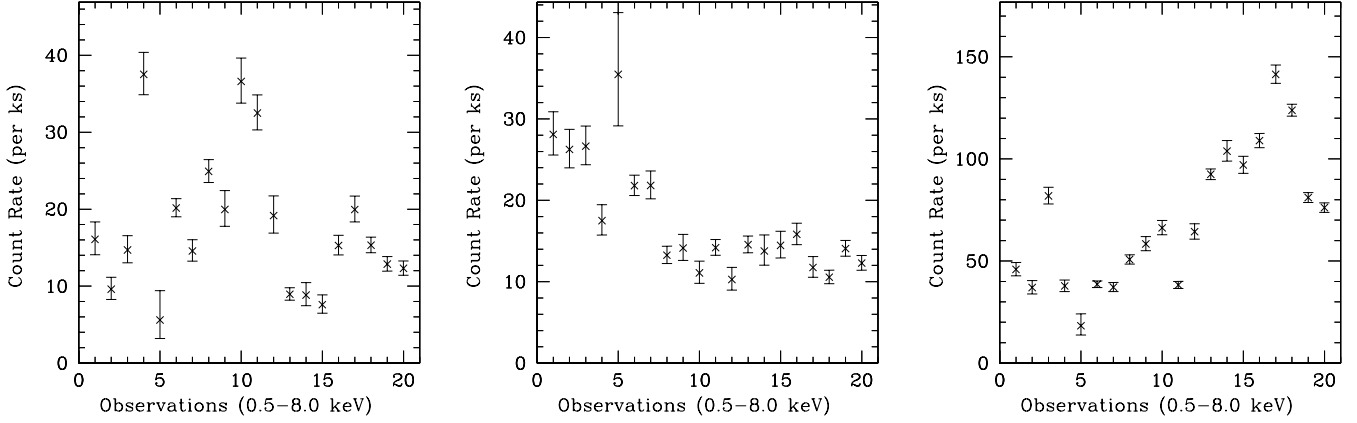


Fig. 6. Count rate (per ks) versus observation number for three example sources. Note that the count rates have been corrected for vignetting. **Left:** CXOHDFN 123612.0+621139, a Seyfert 1.9 galaxy with $z = 0.275$, $L_X = 4 \times 10^{42} \text{ erg s}^{-1}$. CXOHDFN 123618.0+621635, a narrow emission-line ([OIII] only) galaxy with $z = 0.679$, $L_X = 4 \times 10^{43} \text{ erg s}^{-1}$. **Right:** CXOHDFN 123752.7+621628, a BLAGN with $z = 0.307$, $L_X = 2 \times 10^{43} \text{ erg s}^{-1}$.

variable at greater than 99% confidence, respectively. These fractions increase significantly when we restrict ourselves to the 61 objects with > 500 counts (i.e., $\sim 80\%$ and $\sim 90\%$, respectively) or the 27 objects with broad lines (i.e., $\sim 66\%$ and $\sim 92\%$, respectively). The latter results are most likely a result of better photon statistics alone, suggesting that the vast majority of the CDF-N AGN are variable. We detect maximum and median variability amplitudes in the vignetting-corrected count rate of ≈ 7.8 and ≈ 1.9 , respectively, with 3 (15) sources having maximum variability amplitudes larger than 5 (3). The variability properties of these moderate-luminosity AGN are consistent with local studies of Seyfert galaxies (e.g., Nandra et al., 1997a).

ACKNOWLEDGEMENTS

We gratefully acknowledge the financial support of NSF CAREER award AST-9983783 (FEB, CV, DMA, WNB), NASA grant NAS 8-38252 (GPG, PI), NASA GSRP grant NGT5-50247 (AEH), and NSF grant AST-9900703 (DPS). This work would not have been possible without the support of the entire *Chandra* and ACIS teams.

References

- Alexander, D. M., F. E. Bauer, W. N. Brandt, et al. The *Chandra* Deep Field North Survey. XIV. X-ray detected obscured AGNs and starburst galaxies in the bright submm source population. *Astron. J.*, 2003, in press.
- Alexander, D. M., F. E. Bauer, W. N. Brandt, et al. The *Chandra* Deep Field North Survey. XV. 2 Ms source catalogs. *Astron. J.*, 2003, submitted.
- Alexander, D. M., W. N. Brandt, A. E. Hornschemeier, et al. The *Chandra* Deep Field North Survey. VI. The nature of the optically faint X-ray source population. *Astron. J.*, **122**, 2156–2176, 2001.
- Almaini, O., A. Lawrence, T. Shanks, et al. X-ray variability in a deep, flux-limited sample of QSOs. *Mon. Not. R. Astron. Soc.*, **315**, 325–336, 2000.
- Arnaud, K. A. XSPEC: The first ten years. In *ASP Conf. Ser. 101: Astronomical Data Analysis Software and Systems V*, volume 5, pp. 17–20, 1996.
- Barger, A. J., L. L. Cowie, W. N. Brandt, et al. X-ray, optical, and infrared imaging and spectral properties of the 1 Ms *Chandra* Deep Field North sources. *Astron. J.*, **124**, 1839–1885, 2002.
- Barger, A. J., L. L. Cowie, R. F. Mushotzky, et al. The nature of the hard X-ray background sources: optical, near-infrared, submillimeter, and radio properties. *Astron. J.*, **121**, 662–682, 2001.
- Bassani, L., M. Dadina, R. Maiolino, et al. A three-dimensional diagnostic diagram for Seyfert 2 galaxies: probing X-ray absorption and Compton thickness. *Astrophys. J. Supp.*, **121**, 473–482, 1999.
- Bauer, F. E., C. Vignali, D. M. Alexander, et al. X-ray spectral analysis from the *Chandra* Deep Fields.

- Astron. J.*, 2003, in preparation.
- Brandt, W. N., D. M. Alexander, A. E. Hornschemeier, et al. The *Chandra* Deep Field North Survey. V. 1 Ms source catalogs. *Astron. J.*, **122**, 2810–2832, 2001.
- Brandt, W. N., S. Mathur, and M. Elvis. A comparison of the hard ASCA spectral slopes of broad- and narrow-line Seyfert 1 galaxies. *Mon. Not. R. Astron. Soc.*, **285**, L25–L30, 1997.
- Cohen, J. G., D. W. Hogg, R. Blandford, et al. Caltech Faint Galaxy Redshift Survey. X. A redshift survey in the region of the Hubble Deep Field North. *Astrophys. J.*, **538**, 29–52, 2000.
- Comastri, A., G. Setti, G. Zamorani, et al. The contribution of AGNs to the X-ray background. *Astron. & Astrophys.*, **296**, 1–12, 1995.
- Dawson, S., D. Stern, A. J. Bunker, et al. Serendipitously detected galaxies in the Hubble Deep Field. *Astron. J.*, **122**, 598–610, 2001.
- George, I. M., T. J. Turner, T. Yaqoob, et al. X-ray observations of optically selected, radio-quiet quasars. I. The ASCA results. *Astrophys. J.*, **531**, 52–80, 2000.
- Grupe, D., H.-C. Thomas, and K. Beuermann. X-ray variability in a complete sample of Soft X-ray selected AGN. *Astron. & Astrophys.*, **367**, 470–486, 2001.
- Iwasawa, K. and Y. Taniguchi. The X-ray Baldwin effect. *Astrophys. J. Lett.*, **413**, L15–L18, 1993.
- Lawson, A. J. and M. J. L. Turner. GINGA observations of the X-ray spectra of quasars. *Mon. Not. R. Astron. Soc.*, **288**, 920–944, 1997.
- Maiolino, R., M. Salvati, L. Bassani, et al. Heavy obscuration in X-ray weak AGNs. *Astron. & Astrophys.*, **338**, 781–794, 1998.
- Manners, J., O. Almaini, and A. Lawrence. The X-ray variability of high-redshift QSOs. *Mon. Not. R. Astron. Soc.*, **330**, 390–398, 2002.
- Matt, G., A. C. Fabian, M. Guainazzi, et al. The X-ray spectra of Compton-thick Seyfert 2 galaxies as seen by BeppoSAX. *Mon. Not. R. Astron. Soc.*, **318**, 173–179, 2000.
- Mushotzky, R. F., L. L. Cowie, A. J. Barger, et al. Resolving the extragalactic hard X-ray background. *Nature*, **404**, 459–464, 2000.
- Nandra, K., I. M. George, R. F. Mushotzky, et al. ASCA observations of Seyfert 1 galaxies. I. Data analysis, imaging, and timing. *Astrophys. J.*, **476**, 70–82, 1997a.
- Nandra, K., I. M. George, R. F. Mushotzky, et al. ASCA Observations of Seyfert 1 Galaxies. II. Relativistic Iron K alpha Emission. *Astrophys. J.*, **477**, 602–622, 1997b.
- Nandra, K., I. M. George, R. F. Mushotzky, et al. On the Dependence of the Iron K-Line Profiles with Luminosity in Active Galactic Nuclei. *Astrophys. J. Lett.*, **488**, L91–L94, 1997c.
- Nandra, K. and K. A. Pounds. GINGA observations of the X-ray spectra of Seyfert galaxies. *Mon. Not. R. Astron. Soc.*, **268**, 405–429, 1994.
- Reeves, J. N. and M. J. L. Turner. X-ray spectra of a large sample of quasars with ASCA. *Mon. Not. R. Astron. Soc.*, **316**, 234–248, 2000.
- Risaliti, G., M. Elvis, and F. Nicastro. Ubiquitous variability of X-ray-absorbing column densities in Seyfert 2 galaxies. *Astrophys. J.*, **571**, 234–246, 2002.
- Risaliti, G., R. Maiolino, and M. Salvati. The distribution of absorbing column densities among Seyfert 2 galaxies. *Astrophys. J.*, **522**, 157–164, 1999.
- Rosati, P., P. Tozzi, R. Giacconi, et al. The *Chandra* Deep Field-South: The 1 million second exposure. *Astrophys. J.*, **566**, 667–674, 2002.
- Smith, D. A. and C. Done. Unified theories of active galactic nuclei: a hard X-ray sample of Seyfert 2 galaxies. *Mon. Not. R. Astron. Soc.*, **280**, 355–377, 1996.
- Turner, T. J., I. M. George, K. Nandra, et al. ASCA observations of type 2 Seyfert galaxies. II. The importance of X-ray scattering and reflection. *Astrophys. J.*, **488**, 164–173, 1997.
- Turner, T. J., I. M. George, K. Nandra, et al. On X-Ray Variability in Seyfert Galaxies. *Astrophys. J.*, **524**, 667–673, 1999.
- Vignali, C., F. E. Bauer, D. M. Alexander, et al. The *Chandra* Deep Field-North Survey. XVI. The X-ray properties of moderate-luminosity active galaxies at $z > 4$. *Astrophys. J. Lett.*, **580**, L105–L109, 2002.